Check for updates

The Meteoritical Society

Meteoritics & Planetary Science 60, Nr 10, 2359–2375 (2025)
doi: 10.1111/maps.70043

Isotopic analysis of tochilinite (carbonate and magnetite) in Winchcombe: Temperature constraints on early-stage aqueous alteration in the CM parent body

M. D. SUTTLE[1,2]*, R. FINDLAY[1,3], I. A. FRANCHI[1], C. BIAGIONI[2,4], X. ZHAO[1], F. A. J. ABERNETHY[1], L. RICHES[1], and L. FOLCO[2,4]

[1]School of Physical Sciences, The Open University, Walton Hall, Milton Keynes, UK
[2]Dipartimento di Scienze della Terra, Università di Pisa, Pisa, Italy
[3]Department of Earth Sciences, University of Cambridge, Cambridge, UK
[4]CISUP, Centro per l'Integrazione della Strumentazione dell'Università di Pisa, Pisa, Italy

*Correspondence
M. D. Suttle, School of Physical Sciences, The Open University, Walton Hall, Milton Keynes MK7 6AA, UK.
Email: martin.suttle@open.ac.uk

(*Received 06 May 2025; revision accepted 20 August 2025*)

Abstract–We report the first oxygen isotope measurements of tochilinite ($\delta^{17}O$: $11.0 \pm 2.1‰$, $\delta^{18}O$: $23.5 \pm 4.0‰$ and $\Delta^{17}O$: $-1.1 \pm 1.2‰$) in a CM chondrite (Winchcombe, lithology C [CM2.2/2.3]). We analyzed type-I tochilinite-cronstedtite intergrowths (TCIs)—formed by pseudomorphic replacement of kamacite. Alongside T1 and T2 calcite and magnetite, these secondary phases define a linear trendline in $\delta^{17}O$-$\delta^{18}O$ isotope space with a slope of 0.50, slightly shallower than the mass-dependent slope (0.52). This demonstrates that, in addition to dominant mass-dependent fractionation (controlled by mineral-specific and temperature-dependent equilibrium processes), mass-independent mixing between ^{16}O-rich anhydrous silicates, and ^{16}O-poor water influenced the evolving $\Delta^{17}O$ composition of alteration fluids. Petrographic evidence shows tochilinite and T1 calcite formed early and are closely associated in the alteration sequence. Assuming isotopic equilibrium between these phases, we estimate formation temperatures of approximately 135°C and a $\delta^{18}O_{water}$ value of 28‰. These findings align with previous hydrothermal synthesis experiments and underscore the value of multi-phase isotopic measurements for reconstructing the fluid history of chondritic parent bodies.

INTRODUCTION

Tochilinite is a hydroxy-sulfide mineral belonging to the valleriite group with the general formula: $2Fe_{1-x}S \cdot n(Mg,Fe)(OH)_2$, where $0.08 \leq x \leq 0.28$ and $1.58 \leq n \leq 1.75$ (Gubaidulina et al., 2007; Kakos et al., 1994; Organova et al., 1988). It forms a coherently interstratified two-layer structure composed of alternating tetrahedrally coordinated mackinawite-like metal-sulfide layers and octahedrally coordinated brucite-like metal-hydroxide layers (Mackinnon & Zolensky, 1984; Peng et al., 2009). Charge balance between the negatively charged sulfide layers and the positively charged hydroxide layers results in weak electrostatic bonding. Substitution of Fe for Ni, Mg, Cu, and Cr within the mackinawite-like layers and replacement of Fe by Mg, Al, Ca, Na, and other cations into the metal-hydroxide layers allow for a wide range of naturally occurring compositions (Zolensky & Mackinnon, 1986). Tochilinite very rarely forms macrocrystals (>10 μm) under natural or synthetic synthesis (Peng et al., 2009; Vacher, Truche, et al., 2019). This presents challenges to its study.

Tochilinite forms by low-temperature hydrothermal alteration, and on Earth, it is found within serpentinites (e.g., Dietze & Kontny, 2003; Van de Vusse & Powell, 1983) and skarns (e.g., Muramatsu & Nambu, 1980). By contrast, in extraterrestrial settings, tochilinite occurs abundantly, in fact almost exclusively (approximately <5 vol%; McSween Jr, 1987) within the CM chondrites (e.g., Rubin et al., 2007; Suttle, King, et al., 2021;

© 2025 The Author(s). *Meteoritics & Planetary Science* published by Wiley Periodicals LLC on behalf of The Meteoritical Society.
This is an open access article under the terms of the Creative Commons Attribution License, which permits use, distribution and reproduction in any medium, provided the original work is properly cited.

Tomeoka & Buseck, 1985). Trace concentrations of tochilinite have been reported in the CR chondrites (table 8 in Abreu et al., 2020) and the CI chondrites (figure 3 in Nakamura et al., 2022), and it is inferred as a former phase in the metamorphosed CY chondrites (Suttle, Greshake, et al., 2021). Owing to its limited stability field, the presence of tochilinite potentially provides constraints on the temperature ($T = 120$–160°C) and the composition (alkaline) of the fluid present on the CM parent body during the window of tochilinite formation (e.g., Vacher, Truche, et al., 2019). As a salient example, its plenitude in CM2 chondrites and sparsity in CM1 chondrites provide evidence that the CM1s were aqueously altered at higher temperatures than their CM2 cousins (King et al., 2017).

In CM2 chondrites, tochilinite often occurs in intimate association with cronstedtite (the Fe-rich serpentine end-member), forming nanoscale mixtures termed tochilinite-cronstedtite intergrowths (TCIs) (Mackinnon & Zolensky, 1984; Rubin et al., 2007; Tomeoka & Buseck, 1985). They formed early in the aqueous alteration sequence (from CM2.8 onwards, table 6 in Kimura et al., 2020) and were later reprocessed into Fe-Mg-serpentine as aqueous alteration advanced (Rubin et al., 2007; Suttle, King, et al., 2021). TCIs are absent in the more altered CM1 chondrites (King et al., 2017). Because the phyllosilicate in TCI clumps appears to have evolved during aqueous alteration in a way that traces the cation composition of the parent body fluid, their compositions (specifically the Fe-to-Si ratio expressed as "FeO"/SiO_2 in wt%) have been utilized as a metric for the degree of aqueous alteration experienced by the CM lithology (e.g., Lentfort et al., 2021; Rubin et al., 2007; Suttle, King, et al., 2021; Suttle et al., 2024). Two types of TCI are recognized based upon the precursor phases that they replaced:

1. Type-I TCIs form by the pseudomorphic replacement of kamacite grains, resulting in large (>10 μm), compact, rounded grains containing a relatively high abundance of tochilinite intermixed with minor quantities of cronstedtite, goethite, or magnetite (Palmer & Lauretta, 2011; Pignatelli et al., 2016, 2017; Tomeoka & Buseck, 1985). They tend to be Fe-rich (>40 wt%; Palmer & Lauretta, 2011) because the dominant cation in both the mackinawite-like and brucite-like layers is Fe. Furthermore, they may contain appreciable amounts (>3 wt%) of Cr and Ni (Pignatelli et al., 2017), reflecting inherited cations from the precursor Fe-Ni-metal phase.
2. By contrast type-II TCIs have characteristic fibrous textures and typically form masses within the fine-grained matrix (previously referred to as "clumps" or "Poorly Characterized Phases [PCP]"; e.g., Rubin et al., 2007) or occur as mantles overgrowing other mineral phases, most notably calcite (Vacher et al., 2017). Compositionally, Type-II TCIs have lower Fe contents (<35 wt%; Pignatelli et al., 2017) and higher Mg abundances. They are dominated by Fe-rich serpentines, (primarily cronstedtite) with minor quantities of tochilinite and may show compositional zoning in cation content resulting in predominantly Mg-serpentine-rich cores. Crystallographic evidence and rare occurrences of anhedral grains preserved in the center of these TCI masses demonstrate that anhydrous silicates (olivine and pyroxene) and carbonates were the precursor minerals to type-II TCIs (e.g., Daly et al., 2024; Lee et al., 2014; Pignatelli et al., 2016, 2017; Suttle et al., 2024; Tomeoka & Buseck, 1985). Type-II TCIs are significantly more common than type-I TCIs, reflecting the higher abundance of silicates and carbonates over metal in the unaltered CM3 lithology.

Carbonate minerals in CM chondrites act as sensitive records of the fluid conditions at their time of formation. This is because oxygen self-diffusion in carbonates is very low at the temperatures predicted for CM chondrite alteration, preventing re-equilibration with evolving pore fluids (Farver, 1994; Vacher, Piralla, et al., 2019). The presence of multiple carbonate generations in CM chondrites indicates an episodic alteration history (Vacher et al., 2017), representing discrete periods with characteristic fluid compositions and environmental conditions (e.g., pH, temperature and water-to-rock [W/R] mass ratios) during the alteration sequence (e.g., Lee et al., 2013, 2014; Tyra et al., 2016). First-generation (T1) carbonates formed early in the aqueous alteration sequence, before the main growth window for phyllosilicate and pyrrhotite-troilite group Fe-sulfides (Vacher et al., 2017; Lindgren et al., 2017). They are characterized by overgrowth rims. Notably, T1a calcites have rims of tochilinite, while T1b calcites have rims of Fe-sulfide (pyrrhotite-troilite) or metal (Vacher et al., 2017). Second-generation (T2) calcites formed after the main growth windows for phyllosilicate and sulfides and are therefore characterized by inclusions of Fe-sulfide scattered through their interiors. Oxygen isotope analysis of these individual carbonate generations has been used to place constraints on the temperature range during parent body alteration. This approach employs the (alpha [α]) fractionation factor between calcite and water, and calcite and serpentine (e.g., Lee et al., 2014; Telus et al., 2019; Vacher et al. 2017; Vacher, Piralla, et al., 2019; Verdier-Paoletti et al., 2017). Interestingly, TCIs share a similar ability to record the composition of the parent body fluid at their time of formation and to partially preserve this compositional signature through later protracted alteration (Suttle et al., 2024). However,

19455100, 2025, 10, Downloaded from https://onlinelibrary.wiley.com/doi/10.1111/maps.70043 by CochraneItalia, Wiley Online Library on [15/10/2025]. See the Terms and Conditions (https://onlinelibrary.wiley.com/terms-and-conditions) on Wiley Online Library for rules of use; OA articles are governed by the applicable Creative Commons License

no detailed isotopic investigations of TCIs have been undertaken, and only their chemical compositions have been investigated extensively (e.g., Lentfort et al., 2021). One previous isotopic data point for tochilinite was reported as an isotopographic SIMS measurement from the Murchison meteorite (Sakamoto et al., 2007, supplementary information). However, this measurement was subject to significant and undefined uncertainty and lacked petrographic context.

In this study, we provide the first high precision O-isotope measurement of tochilinite in the CM chondrite Winchcombe (King et al., 2022), using NanoSIMS coupled with a correction on the matrix effect using a terrestrial tochilinite standard. We use these data, combined with O-isotope measurements on calcite and magnetite, to quantitatively constrain the ambient alteration temperatures on the CM chondrite parent body during early-stage aqueous alteration, prior to the formation of phyllosilicate.

METHODS

Samples

We studied tochilinite (carbonates and magnetite) within a single resin-mounted polished section of the Winchcombe meteorite, a CM2 chondrite (from the Natural History Museum, London [NHM], with section ID: P30423 and accession number: BM.2022, M1-87). This section samples part of the main mass recovered from the residential driveway (King et al., 2022; Russell et al., 2023). It is approximately ~40.2 mm^2 in exposed area and is composed exclusively of the Lithology C material, as defined in Suttle et al. (2024). This lithology was assigned a petrologic grade of CM2.2/2.3, reflecting moderate-to-advanced aqueous alteration. Within this section, three grains of near-pure tochilinite were previously identified (figure 2b of Suttle et al., 2024).

In addition, we studied a single sample of terrestrial tochilinite, collected from the Otamo Quarry, based in Siikainen, Finland. At this site tochilinite occurs as thin platy crystals, up to 5 mm across, bronze-black in color, associated with dolomite. This sample was made available by the mineral collector Ulf Nyberg. Additional information on this locality can be found in Sandström (2012). Owing to the relatively small amount of pure tochilinite, our identification was confirmed using X-ray powder diffraction collected in a Gandolfi-like geometry using a Bruker D8 Venture single-crystal X-ray diffractometer equipped with a Photon III CCD area detector and microfocus Cu$K\alpha$ radiation (instrument based at the Centro per l'Integrazione della Strumentazione scientifica dell'Università di Pisa, CISUP, University of Pisa, Italy). Observed X-ray diffraction lines from this sample are reported in Table S1.

Petrographic Characterization

We used scanning electron microscope (SEM), backscattered electron (BSE) imaging, and energy dispersive spectroscopy (EDS) to characterize the texture and chemical composition of the tochilinite grains. This was performed at the Open University (OU) using a TESCAN Clara SEM. This SEM is fitted with an Oxford Instruments UltimMax 170 mm^2 detector and provides "standardless" EDS data calibrated to the Oxford Instruments "Extended Factory Set" (in-factory using a collection of pure elemental standards). Prior to analysis, we performed energy channel calibration (peak position and intensity) using a pure copper metal reference. All spot analyses were performed at high-vacuum, with an accelerating voltage of 20 kV, a beam current of 1.5 nA, and a fixed optimal working distance (10 mm). We used the Oxford Instruments AZtec software (version 6.1 HF3). Acquisition settings were as follows: "process time 4," 2048 energy channels, and a live acquisition time of 20 s. Resulting quantitative EDS data were processed with standard XPP matrix correction routines (Pouchou & Pichoir, 1991). We applied the "all elements" quantification routine, meaning that no *apriori* assumptions are made on the anion composition of the sample, and therefore the abundance of all elements (including oxygen) was determined from their individual K/L peak intensities. All geochemical data are quoted as uncorrected weight totals (wt%) and given to one decimal place (Table 1).

After SEM analysis, the carbon coat was removed and the tochilinite masses were analyzed with Raman spectroscopy to confirm their phase identification as tochilinite. We used a Horiba Jobin-Yvon LabRam HR Raman microscope, located at the OU. Analyses were performed using a 514 nm (green) laser and a 100× long working distance objective lens, giving a beam diameter of ~2 μm. Spectra were collected for three cycles of between 60 and 120 s with a 600 grooves/mm grating and a backlit CCD detector. Laser power at the sample surface was <50 μW in order to prevent damage to the grains. The resulting spectra were compared against a tochilinite spectrum obtained from the RRUFF database (RRUFF ID: R060887).

O-isotope Measurements—Developing A Terrestrial Tochilinite Standard

All O-isotope data presented in this study are quoted in ‰ and given in relation to VSMOW. We measured the O-isotope composition of the Winchcombe tochilinite using a Cameca NanoSIMS 50 L based at the OU.

19455100, 2025, 10, Downloaded from https://onlinelibrary.wiley.com/doi/10.1111/maps.70043 by CochraneItalia, Wiley Online Library on [15/10/2025]. See the Terms and Conditions (https://onlinelibrary.wiley.com/terms-and-conditions) on Wiley Online Library for rules of use; OA articles are governed by the applicable Creative Commons License

TABLE 1. Chemical compositions of tochilinite grains studied in this work.

Location	Figure	Analysis	N = -?	Na	Mg	Al	Si	P	S	Cr	Mn	Fe	Co	Ni	O	Total	Notes
Extraterrestrial: Winchcombe, lithology C (CM2.2/2.3)	Figure 1a	Avg.	3	0.6	4.2	0.3	2.5	0.4	18.5	3.1	0.2	34.8	0.1	2.0	26.0	92.7	Large (>100 μm), round grain, with Ni-rich rim
		Stdev.		0.1	0.2	0.1	0.1	0.1	0.9	0.1	0.2	0.4	0.2	0.3	1.3	1.3	
	Figure 1b	Avg.	3	0.8	5.5	0.5	6.1	0.7	10.0	2.7	0.3	27.7	—	4.3	35.5	94.1	Small (~25 μm), round grain, with magnetite rim
		Stdev.		0.1	0.7	0.1	0.7	0.1	1.9	0.5	0.1	1.4	0.1	0.4	4.3	5.2	
	Figure 1c	Avg.	4	—	3.8	0.3	2.2	0.8	16.8	2.7	0.1	33.3	0.1	6.4	25.8	92.4	Large (>50 μm), irregular-shaped grain, with Ni-rich rim
		Stdev.		—	1.2	0.1	0.6	1.1	4.3	1.4	0.2	3.4	0.2	9.4	6.3	1.9	
Terrestrial: Otamo quarry, Finland	Figure 1d–f	Avg.	5	—	11.4	—	—	—	22.8	—	—	46.9	—	—	20.7	101.7	EDS on external surface (only)
		Stdev.		—	0.3	—	—	—	2.0	—	—	10.6	—	—	6.9	11.1	

Note: Data are averaged spot EDS analyses, presented as uncorrected weight totals and quoted to 1 d.p. precision. Their compositions can be correlated with the grains shown in Figure 1.

19455100, 2025, 10, Downloaded from https://onlinelibrary.wiley.com/doi/10.1111/maps.70043 by Cochraneltalia, Wiley Online Library on [15/10/2025]. See the Terms and Conditions (https://onlinelibrary.wiley.com/terms-and-conditions) on Wiley Online Library for rules of use; OA articles are governed by the applicable Creative Commons License

However, appropriate corrections must be applied to any of the raw NanoSIMS data to account for artifacts that introduce inaccuracies in the measured isotopic composition of a given mineral phase. Most significantly, we must account for (1) matrix effects arising because the chemical composition, crystallography, and sputtering behavior of the target mineral impact the efficiency of secondary ionization and emission and (2) instrumental mass fractionation effects that arise as different mass ions are systematically influenced by the instrument's electromagnetic fields (e.g., Riciputi et al., 1998). To overcome these issues, we apply correction factors determined by applying calibration factors based on the measurement of mineral standards, whose isotopic compositions are known independently. These corrections ensure that the measured isotopic ratios on the sample accurately reflect the true isotopic composition of the target mineral phase (e.g., Hauri et al., 2016; Scicchitano et al., 2018).

To date, the absence of a readily available and well-characterized terrestrial isotopic tochilinite standard has prevented the quantitative isotopic analysis of tochilinite in CM chondrites. However, we were able to acquire a sufficient quantity of terrestrial tochilinite from the Otamo Quarry for this work. The triple oxygen isotope composition of the terrestrial Otamo quarry tochilinite was determined at the OU, using our bespoke infrared laser-assisted fluorination mass spectrometry instrument (outlined in Miller et al., 1999). We measured 341 μg of tochilinite using the modified single-shot laser fluorination method (outlined in Greenwood et al., 2023, 2024).

The Otamo quarry tochilinite was loaded as a single sample into a nickel tray alongside two obsidian standards (one large, one small). The advantage of only loading one unknown is that it prevents the possible pre-reaction of tochilinite with BrF_5 at room temperature. The analysis tray was sealed between two knife edges using a copper gasket and allowed to pump to a high vacuum overnight at 80°C. The following day, the tochilinite was reacted in the presence of BrF_5 using a 50 W CO_2 fusion laser. Tochilinite has a modest oxygen budget (approximately 10–15 wt%), all of which is located as hydroxyl molecules with the octahedrally coordinated brucite-like layers.

The combination of a low oxygen budget and a small sample mass (<1 g) necessitated a microvolume analysis followed by a blank correction applied to the data (Greenwood et al., 2024). The blank correction was calculated by assessing the deviation of the small obsidian standard from the known value. The resulting composition of the terrestrial Otamo Quarry tochilinite reported from the laser line was: $\delta^{17}O$: −2.03‰, $\delta^{18}O$: −3.65‰, and $\Delta^{17}O$: −0.13‰. System precision for small analyses, as defined by repeat, small (0.12 mg) blank corrected analyses ($N = 21$) of the OU obsidian standard is: ±0.094‰ for $\delta^{17}O$; ±0.163‰ for $\delta^{18}O$; ±0.018‰ for $\Delta^{17}O$ (2σ) (Greenwood et al., 2024).

NanoSIMS Measurements (Tochilinite, Carbonate and Magnetite)

The in situ O-isotope composition of target phases was analyzed using a CAMECA NanoSIMS 50 L based at the OU. Prior to analysis, each area of interest was pre-sputtered with a 100 pA Cs^+ probe for 3 min over an area of 7 × 7 μm to remove the carbon coat, any potential surface contamination, and to achieve sputter equilibrium. Analyses were performed with a 100 pA Cs^+ probe rastered over a 5 × 5 μm region in "spot" mode. An electron "flood gun" was used for charge compensation. Seven different secondary ion species were collected simultaneously, with $^{16}O^-$ measured on a Faraday detector, while $^{17}O^-$, $^{18}O^-$, $^{30}Si^-$, $^{24}Mg^{16}O^-$, $^{40}Ca^{16}O^-$, and $^{56}Fe^{16}O^-$ were measured on electron multipliers. The stated mass resolving power is ∼10,000 (CAMECA definition, based on the measured peak width between 10% and 90% of the peak), sufficient to resolve the $^{16}OH^-$ interference from $^{17}O^-$.

Analyses lasted approximately 7 min, providing a total of (1.5–2.0) x 10^{10} counts for the $^{16}O^-$ isotope. Standard samples of NHM calcite ($\delta^{18}O$: 15.47‰; Tomkinson, 2012), magnetite ($\delta^{18}O$: 6.47‰), and terrestrial tochilinite ($\delta^{18}O$: −3.65‰) were analyzed before and after each block of unknown samples to correct the instrumental mass fractionation. Analytical uncertainty (all 2σ), incorporating internal precision and external precision from standard replicates, is typically ±1.3‰ for $\delta^{17}O$, ±1.0‰ for $\delta^{18}O$ and approximately ±1.0‰ for $\Delta^{17}O$. Analyses of the extraterrestrial (Winchcombe) tochilinite were subject to much higher $^{16}OH^-$ signal than calcite and magnetite grains. In such circumstances, the mass resolving power employed results in a small contribution of $^{16}OH^-$ to the $^{17}O^-$ signal. To correct for this interference, the $^{16}OH^-$ signal was measured for 10 seconds at the start and end of each measurement, and the $\delta^{17}O$ adjusted according to a calibration of $\Delta^{17}O$ versus the measured $^{16}OH^-/^{17}O^-$ intensity determined by analyses of terrestrial tochilinite and San Carlos olivine.

All NanoSIMS O-isotope measurements on Winchcombe tochilinite, carbonate, and magnetite collected in this study are given in Table 2.

RESULTS

Petrography

The Winchcombe tochilinite analyzed in this study occurs as three small (<200 μm) dense and homogenous

19455100, 2025, 10, Downloaded from https://onlinelibrary.wiley.com/doi/10.1111/maps.70043 by CochraneItalia, Wiley Online Library on [15/10/2025]. See the Terms and Conditions (https://onlinelibrary.wiley.com/terms-and-conditions) on Wiley Online Library for rules of use; OA articles are governed by the applicable Creative Commons License

TABLE 2. Oxygen isotope compositions of tochilinite, carbonates (T1 and T2) and magnetite from Winchcombe lithology C.

Phase	Grain	$\delta^{17}O$	2σ	$\delta^{18}O$	2σ	$\Delta^{17}O$	2σ
Tochilinite	Large 165 μm grain (Figure 1a)	9.0	1.2	20.6	1.0	−1.8	1.2
		10.0	1.2	19.5	1.0	−0.1	1.2
		11.8	1.3	27.2	1.1	−2.3	1.2
		13.8	1.2	26.6	1.0	0.0	1.2
	Avg.	11.2	—	23.5	—	−1.1	—
	SD	2.13	—	4.00	—	1.16	—
T1 calcite	Grain 1	21.9	0.9	40.9	0.5	0.7	1.0
		18.6	0.9	35.6	0.5	0.1	1.0
	Grain 2	21.4	0.9	40.5	0.5	0.4	1.0
		20.6	0.9	39.9	0.5	−0.1	1.0
		20.1	0.9	39.2	0.5	−0.3	1.0
		21.8	1.0	42.2	0.5	−0.2	1.0
	Grain 3	21.9	1.0	41.6	0.5	0.2	1.0
		23.0	0.9	42.6	0.5	0.9	1.0
		23.2	1.0	42.5	0.5	1.1	1.0
	Grain 4	20.0	1.0	39.6	0.5	−0.6	1.0
	Avg.	21.3	—	40.5	—	0.2	—
	SD	1.43	—	2.11	—	0.55	—
T2 calcite	Grain 1	17.3	1.2	33.7	0.7	−0.2	1.0
		15.0	1.2	31.0	0.6	−1.2	1.0
		16.9	1.2	35.0	0.7	−1.2	1.0
	Avg.	16.4	—	33.2	—	−0.9	—
	SD	1.24	—	2.01	—	0.56	—
Magnetite	Grain 1	−5.0	0.9	−12.3	0.5	1.4	1.0
		−4.8	0.9	−11.2	0.5	1.0	1.0
		−5.7	0.9	−13.7	0.5	1.4	1.0
		−6.2	1.1	−10.8	0.7	−0.6	1.0
		−4.6	1.1	−8.9	0.7	0.0	1.0
	Grain 2	−3.9	0.9	−11.2	0.5	1.9	1.0
		−3.7	0.8	−11.6	0.4	2.3	1.0
	Avg.	−4.9	—	−11.4	—	1.1	—
	SD	0.91	—	1.45	—	1.04	—

Note: Data are displayed in permille (‰) and quoted relative to VSMOW. Uncertainties given in the "2σ" column represent analytical uncertainties quoted at the 2× standard deviation level. For each phase, the average composition and standard deviation (arising exclusively from intrasample variation and not accounting for analytical uncertainty) are quoted as labeled rows.

grains, containing abundant radial fractures (Figure 1). Raman spectra, collected after removal of the carbon coat (Figure S1) confirm our phase identification as tochilinite, having characteristic peaks centered at 235, 300, and 360 cm^{-1}, which match that of terrestrial tochilinite measured under the same conditions.

The Winchcombe tochilinite masses have approximate diameters of 165 μm (Figure 1a), 25 μm (Figure 1b) and 90 μm (Figure 1c). Two of these grains have rounded shapes (Figure 1a,b), while the third can be approximated to a rectangle in section view (Figure 1c). Two of the grains have well-defined, thin (<15 μm) Ni-rich rims, with Ni contents up to 21 wt%. In addition, two of the grains have mantles containing magnetite (occurring either as equant grains or as framboids) intermixed with small (<10 μm) rounded Ca-carbonate (calcite) grains. Spot EDS analyses on the tochilinite (Table 1) revealed compositions containing (in order of abundance): O (24.2–39.8 wt%), Fe (26.5–35.4), S (8.1–19.7 wt%), Mg (3.9–6.2 wt%), Si (2.4–6.8 wt%), Cr (2.3–3.4 wt%), and Ni (1.6–4.6 wt%), with trace quantities (<0.8 wt%) of Na, Al, P, Mn, and Co. EDS weight totals on tochilinite are low (<90 wt%). The missing mass is attributed to artifacts (porosity and minor beam overlap effects) and the inability to detect hydrogen. All three grains have similar compositions (Table 1) although the smallest grain (Figure 1b) contains elevated Si contents (6.1 ± 0.7 wt%), indicating nanoscale intermixed cronstedtite. The average tochilinite composition ($N = 10$), based on data from all three

19455100, 2025, 10, Downloaded from https://onlinelibrary.wiley.com/doi/10.1111/maps.70043 by CochraneItalia, Wiley Online Library on [15/10/2025]. See the Terms and Conditions (https://onlinelibrary.wiley.com/terms-and-conditions) on Wiley Online Library for rules of use; OA articles are governed by the applicable Creative Commons License

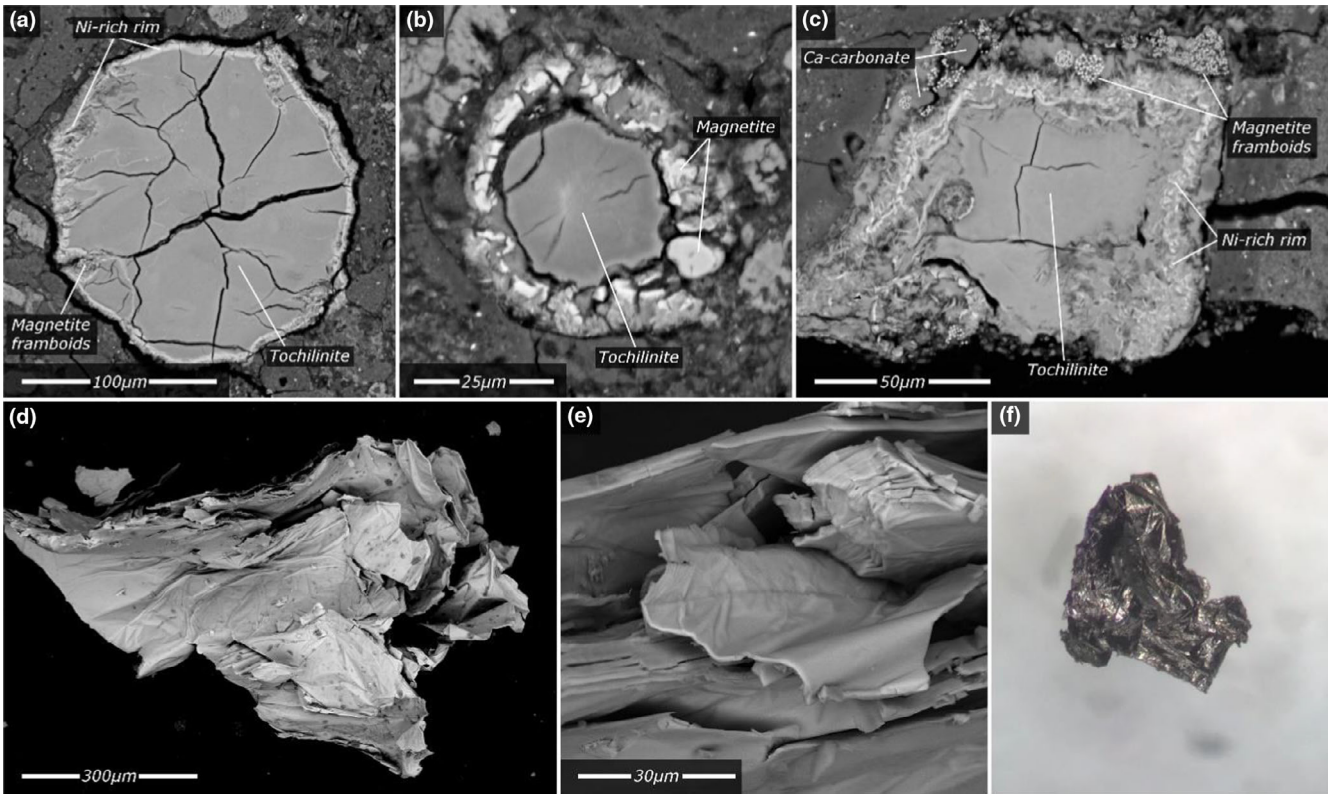

FIGURE 1. Textures of the tochilinite grains analyzed in this study, shown in BSE (a–e) and under optical microscope (f). Panels (a–c) depict tochilinite found in Winchcombe's lithology C (Suttle et al., 2024). They are type-I TCIs, formed by the pseudomorphic replacement of Fe-Ni-metal (kamacite) grains (Palmer & Lauretta, 2011; Pignatelli et al., 2017) and contain Ni-rich rims, reflecting the concentration of Ni along the grain's perimeter formed during fluid-induced replacement (Ni being less compatible within the tochilinite structure than Fe). In panels (b) and (c), the tochilinite masses are mantled by magnetite (either as equant grains or framboids), and Ca-carbonates (calcite). All three tochilinite masses have large radial fractures. Panels (d–f) depict a sample of pure terrestrial tochilinite (>500 μm in length) with its characteristic fibrous habit (e). Pure tochilinite appears a dull metallic gray color in optical light with a texture similar to crumpled "tin-foil" (f). (Color figure can be viewed at wileyonlinelibrary.com)

grains, is: 32 wt% Fe, 29 wt% O, 15 wt% S, 5 wt% Mg, 4 wt% Si, 4 wt% Ni, and 3 wt% Cr. The terrestrial tochilinite standard has a similar composition (Table 1) but is Mg-enriched (Mg: 11.4 ± 0.3 wt%) and Fe-rich (Fe: 49.9 ± 10.6 wt%) and, correspondingly, contains no detectable Ni, Cr, and Si, which are otherwise found at >1.5 wt% level in the Winchcombe tochilinite. Thus, the morphology (rounded, isolated grains embedded within the fine-grained matrix) combined with the presence of Ni and Cr and low Si content is consistent with the descriptions of type-I TCIs previously reported in CM chondrites (e.g., Palmer & Lauretta, 2011; Pignatelli et al., 2016, 2017; Tomeoka & Buseck, 1985).

Winchcombe's lithology C also contains carbonates and magnetite. These phases are studied to provide additional context that supports the interpretation of the O-isotope composition of the measured tochilinite grains. Carbonates are found only as calcite and occur across multiple generations. T1 calcites are overwhelmingly the dominant type, while T2 calcites are rare. A third generation consists of dense clusters of small (1–20 μm), ellipsoidal calcite grains that are closely associated with magnetite. These typically infill cracks, fractures, and vugs, as described in Suttle et al. (2024).

Magnetite appears in two forms. Rare, large polyhedral grains with subhedral morphologies and rippled textures are the most prominent expression (Figure 2). All of these large magnetite grains are mixed-phase, containing Fe-sulfide (pentlandite) either as inclusions or as clusters along grain margins. Magnetite also occurs as framboids within the fine-grained matrix and in association with the small carbonate grains (e.g., Figures 1 and 2).

Tochilinite O-Isotope Composition

Four O-isotope measurements were collected from the largest tochilinite grain (Figure 1a, Figure S2). Compositions range from $\delta^{17}O$: 9.0–13.8‰, $\delta^{18}O$: 19.5–27.2‰, and $\Delta^{17}O$: −2.3–0.0‰. The analytical

19455100, 2025, 10, Downloaded from https://onlinelibrary.wiley.com/doi/10.1111/maps.70043 by CochraneItalia, Wiley Online Library on [15/10/2025]. See the Terms and Conditions (https://onlinelibrary.wiley.com/terms-and-conditions) on Wiley Online Library for rules of use; OA articles are governed by the applicable Creative Commons License

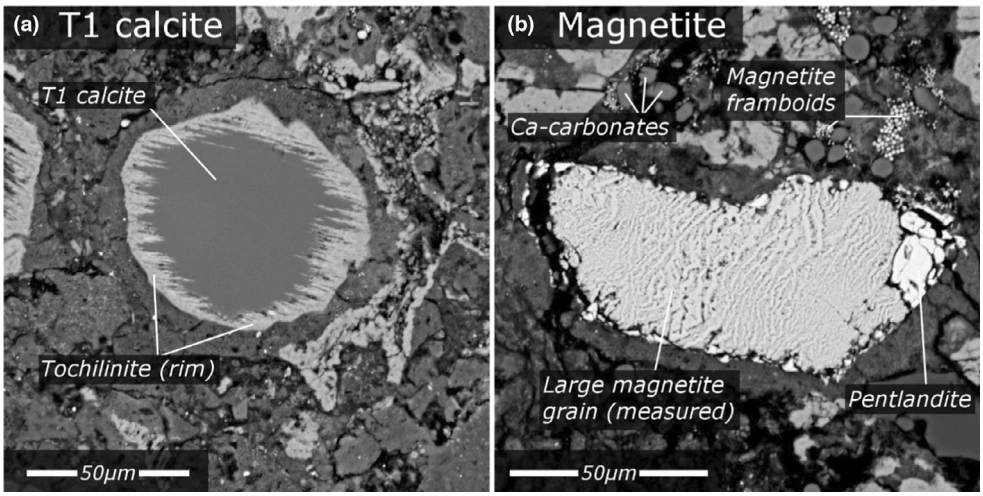

FIGURE 2. Example images of (a) T1 calcite and (b) magnetite grains measured in this study for O-isotopes. (a) T1 calcite grains are common in Winchcombe's lithology C and appear as small, euhedral grains with uniform composition and an absence of fractures, pores, or inclusions. They have well-developed rims of TCI material (labeled here as tochilinite for simplicity) which penetrate into the calcite core, exploiting the microstructure of the host calcite during progressive replacement. (b) Rare large magnetite grains are present in Winchcombe's lithology C. They have subhedral morphologies with rippled textures and a close association with Ni-rich Fe-sulfide (pentlandite). This texture is interpreted as incomplete replacement of Fe-sulfide by magnetite during aqueous alteration. Most likely, the low-Ni sulfide (pyrrhotite-troilite) has been replaced while the more resistant pentlandite remains. Magnetite is also present as smaller framboids, which occur abundantly across the sample interstitially within the matrix and in close association with small euhedral Ca-carbonate grains.

uncertainty at the 2σ level is $\pm 1.3‰$, $\pm 1.1‰$ and $\pm 1.2‰$ (2σ) respectively for $\delta^{17}O$, $\delta^{18}O$, and $\Delta^{17}O$ (Figure 3 and Table 2). These values give an averaged tochilinite composition of$\delta^{17}O$: $11.0 \pm 2.1‰$, $\delta^{18}O$: $23.5 \pm 4.0‰$, and $\Delta^{17}O$: $-1.1 \pm 1.2‰$, where the quoted uncertainties for the average composition are given to 1 SD.

Carbonate O-Isotope Compositions

We collected O-isotope data (Table 2 and Figure 3) on a suite of carbonates in the same Winchcombe section (Figure S3). Owing to their abundance within lithology C, we focus on the T1a calcites (hereafter referred to as T1 calcite). We measured 10 spots on four different T1 calcite grains. They have averaged compositions of: $\delta^{17}O$: $21.3 \pm 1.4‰$, $\delta^{18}O$: $40.5 \pm 2.1‰$, and $\Delta^{17}O$: $0.2 \pm 0.6‰$, where the quoted uncertainties here are 1 SD (individual spot data are given in Table 2).

In addition, we measured three spots on a single (T2) calcite grain; these averaged: $\delta^{17}O$: $16.4 \pm 1.2‰$, $\delta^{18}O$: $33.2 \pm 2.0‰$, and $\Delta^{17}O$: $-0.9 \pm 0.6‰$, where the quoted uncertainties here are 1 SD (individual spot data are given in Table 2).

Magnetite O-Isotope Compositions

We collected O-isotope data (Table 2 and Figure 3) on two large polyhedral magnetite grains within lithology C (in total seven spots). They give an average value of $\delta^{17}O$: $-4.9 \pm 0.9‰$, $\delta^{18}O$: $-11.4 \pm 1.5‰$, and $\Delta^{17}O$: $1.1 \pm 1.0‰$, where the quoted uncertainties here are 1 standard deviation (individual spot data are given in Table 2).

DISCUSSION

Section 1: The $\Delta^{17}O$ Composition of Winchcombe's Parent Body Fluid

We evaluated the distribution of our entire O-isotope dataset (tochilinite, carbonates, and magnetite), calculated a line-of-best-fit, and used this to test whether all the secondary phases could be defined by a single linear trendline in $\delta^{17}O$-$\delta^{18}O$ isotope space. If so, the slope of this line would define the inferred $\Delta^{17}O$ composition of the fluid phase during secondary mineral formation.

We used orthogonal distance regression (ODR) for the fitting process because it accounts for analytical uncertainties in both $\delta^{17}O$ and $\delta^{18}O$ values. Our line-of-best-fit yields a slope of 0.50 ± 0.01 and an R^2 coefficient of determination of 0.99 (Figure 3, Table 3). This was evaluated further by statistical testing using a t-test applied to the ODR-estimated slope parameter, comparing it against a hypothesized slope value of 0.52 (reflecting a mass-dependent process) and using the ODR-derived

19455100, 2025, 10, Downloaded from https://onlinelibrary.wiley.com/doi/10.1111/maps.70043 by CochraneItalia, Wiley Online Library on [15/10/2025]. See the Terms and Conditions (https://onlinelibrary.wiley.com/terms-and-conditions) on Wiley Online Library for rules of use; OA articles are governed by the applicable Creative Commons License

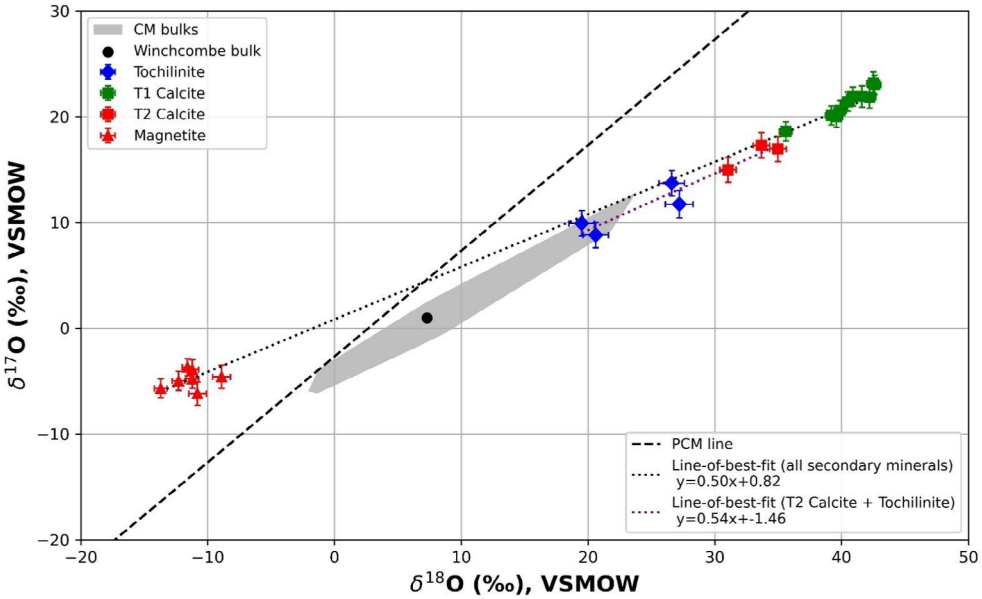

FIGURE 3. The O-isotope composition of measured secondary phases (tochilinite [blue diamonds], T1 calcite [dark green squares], T2 calcite [light green squares] and magnetite [red triangles]) in Winchcombe's lithology C (CM2.2/2.3). For all measured NanoSIMS data, 2σ error bars are shown, representing instrumental analytical uncertainty. We fitted a line-of-best-fit (ODR fit) against all our measured secondary phases (marked as a dotted black line). This reveals a slope value of 0.50 ± 0.01 and an R^2 value of 0.99. Another line-of-best-fit against only the tochilinite and T2 calcite data reveals a slope of 0.54 ± 0.06 (within error of a mass-dependent slope) and an R^2 value of 0.99. This suggests that only the tochilinite and T2 calcite formed from a fluid of the same $\Delta^{17}O$ composition and, potentially in isotopic equilibrium. Also shown are data for the Winchcombe bulk composition, which reflects the average composition from several different lithologies in this meteorite (King et al., 2022) (black circle). For reference we include a gray shaded region denoting the range occupied by previous literature measurements of bulk CM chondrite compositions (N = 135). The data used to define this area are from: Clayton and Mayeda (1999), Tyra et al. (2007), Moriarty et al. (2009), Alexander et al. (2018), King et al. (2019), Verdier-Paoletti et al. (2019), Kimura et al. (2020), Lee et al. (2016, 2019), Fan et al. (2022), Greenwood et al. (2024) and The Meteoritical Bulletin (2024) (and shown in Table S2). The dashed black line shows the slope-1 Primary Chondrule Mineral (PCM) line, as defined by Ushikubo et al. (2012). (Color figure can be viewed at wileyonlinelibrary.com)

standard error and n-2 degrees of freedom. Statistical testing confirmed that our trendline is distinct, at the 95% confidence level ($p = 0.0107$), from a mass-dependent slope. Thus, the full suite of Winchcombe's secondary minerals cannot have precipitated from a fluid with uniform $\Delta^{17}O$ composition. Instead, the fluid's $\Delta^{17}O$ composition must have varied over time, requiring that some degree of mass-independent mixing occurred between isotopic reservoirs during aqueous alteration.

This interpretation is consistent with the understanding that aqueous alteration on the CM parent body records water-rock interactions that progressively replaced anhydrous silicates with hydrated phyllosilicates (e.g., Howard et al., 2015). The anhydrous silicates are ^{16}O-rich and plot along a primitive slope-1 line (e.g., the primitive chondrules mineral [PCM] line), while the starting fluid composition was not on this line, but instead at an isotopically heavier value (e.g., Clayton & Mayeda, 1999; Fujiya, 2018; Suttle, King, et al., 2021). As alteration progressed, the $\Delta^{17}O$ composition of the fluid would have evolved. At the same time, secondary phases that precipitated from that fluid would reflect the instantaneous isotopic composition of the water at that point in time but further fractionated by mineral-specific and temperature-dependent (mass-dependent) processes. These processes would cause newly formed secondary minerals to migrate off the anhydrous silicate-water tie-line and along a slope-0.52 trendline. Consequently, any evaluation of the O-isotope composition of secondary minerals in CM chondrites should define a trendline with a slope $\neq 0.52$ if they precipitated from fluids undergoing $\Delta^{17}O$ isotopic evolution (as seen in Figure 3). However, for any given moment in the alteration sequence, when the fluid $\Delta^{17}O$ composition was temporarily static, minerals formed under those conditions may define a slope 0.52 trendline, consistent with isotopic equilibrium and, therefore, subsets of secondary phases may themselves define slope-0.52 trendlines when considered separately from the entire secondary mineral population.

To test which minerals may have formed under such equilibrium conditions, we systematically evaluated all

19455100, 2025, 10, Downloaded from https://onlinelibrary.wiley.com/doi/10.1111/maps.70043 by CochraneItalia, Wiley Online Library on [15/10/2025]. See the Terms and Conditions (https://onlinelibrary.wiley.com/terms-and-conditions) on Wiley Online Library for rules of use; OA articles are governed by the applicable Creative Commons License

TABLE 3. Outcome of ODR fitting and statistical testing on the secondary mineral phase O-isotope compositions in Winchcombe.

Scenario	Phases considered	N =?	Slope	Slope uncertainty	Intercept	Intercept uncertainty	t statistic	p value	R^2	Potentially consistent with 0.52?
0	Tochilinite + T2 Calcite	7	0.5357	0.0637	−1.457	1.8155	0.2459	0.8155	0.9867	Yes
1	T2 Calcite + Magnetite	10	0.4711	0.0156	0.713	0.2852	−3.1424	0.0138	0.9989	No
2	Tochilinite + Magnetite	11	0.4505	0.0198	0.4736	0.3036	−3.4996	0.0067	0.9978	No
3	T1 Calcite + T2 Calcite	13	0.6616	0.041	−5.5186	1.6166	3.4523	0.0054	0.9923	No
4	Tochilinite + T1 Calcite	14	0.5983	0.0254	−2.9497	0.9662	3.0863	0.0094	0.9959	No
5	Tochilinite + T2 Calcite + Magnetite	14	0.4636	0.0131	0.5956	0.254	−4.3163	0.001	0.9986	No
6	T1 Calcite + Magnetite	17	0.4999	0.007	1.0321	0.2211	−2.8874	0.0113	0.9995	No
7	Tochilinite + T1 Calcite + T2 Calcite	17	0.6044	0.0241	−3.2441	0.9048	3.4942	0.0033	0.9953	No
8	T1 Calcite + T2 Calcite + Magnetite	20	0.4974	0.0073	0.9612	0.2328	−3.1027	0.0061	0.9993	No
9	Tochilinite + T1 Calcite + Magnetite	21	0.4988	0.0085	0.8659	0.2649	−2.4841	0.0225	0.9987	No
10	All (full group)	24	0.4967	0.0084	0.8165	0.2607	−2.7883	0.0107	0.9986	No

Note: We considered all potential combinations of secondary phases for the fit and test. A statistical t-test was used to assess whether the calculated slope values are statistically indistinguishable from a reference slope of 0.52. Our results show that, for all combinations except tochilinite + T2 calcite, the best-fit trendlines deviate from a slope of 0.52, indicating that these mineral pairs did not form from a single fluid composition (constant $\Delta^{17}O$ value). In the case of tochilinite + T2 calcite, the slope uncertainty is notably larger (±0.06) compared to other combinations, due to the limited number of data points ($N = 7$). Therefore, while this scenario appears closer to a slope of 0.52, the elevated uncertainty means it too could be distinct from that value.

possible combinations of the four secondary phases (tochilinite, T1 calcite, T2 calcite, and magnetite) and assessed whether any scenario could be described by a linear trendline, consistent with a slope of 0.52. The results (Table 3) indicate that the only combination potentially consistent with formation from a common fluid source is tochilinite and T2 calcite, which yield a trendline slope of 0.54 ± 0.06 ($R^2 = 0.99$, $p = 0.82$). The relatively large uncertainty is due to the small number of data points ($N = 7$), compared to a median of $N = 14$ and a maximum of $N = 24$ across other combinations. While this slope appears broadly consistent with a mass-dependent value (0.52), the limited dataset makes the result statistically ambiguous and highlights the influence of small-number statistics on the interpretation. Thus, we conclude that none of the measured phases appear to have formed in isotopic equilibrium with another phase.

Given the above analysis, we conclude that a combination of both mass-independent mixing (via water-rock fluid interaction between isotopically distinct reservoirs—^{16}O-rich solar-like silicates, formed in the inner Solar System; e.g., Yurimoto et al., 2007) and ^{16}O-poor water-ice condensed in the outer Solar System (e.g., Clayton & Mayeda, 1999) and mass-dependent processing—arising from mineral-specific and temperature-dependent fractionation defines the composition of Winchcombe's secondary phases. But which process was dominant? The observed maximum $\Delta^{17}O$ variation is small (~4.6‰) relative to the much larger $\delta^{18}O$ variation (~56.3‰), and all of our calculated trendlines, regardless of which secondary phases are included (Table 3), have slope values close to 0.52. This implies that mass-dependent fractionation (variable temperature) was the dominant variable controlling the isotopic composition of the secondary phases.

With this knowledge, we can now consider how this isotopic evidence relates to existing petrographic constraints on the sequence of mineralization in CM chondrites. T1 calcite is a well-studied phase; both petrographic (euhedral morphologies, absence of inclusions) and O-isotope evidence (^{16}O-poor compositions) demonstrate that it formed early, as the first major generation of carbonate in CM chondrites (e.g., Lindgren et al., 2017; Vacher et al., 2017). The presence of tochilinite rims on T1 calcite requires that tochilinite (or at least type-II TCIs) formed after T1 calcites. However, the timing of type-I TCIs relative to T1 calcite is less clear. Type-I TCIs formed by metal replacement, and these are the tochilinite morphologies that we have measured in this work. They must also form very early in the alteration sequence. This is because Fe-Ni metal is highly susceptible to attack and

19455100, 2025, 10, Downloaded from https://onlinelibrary.wiley.com/doi/10.1111/maps.70043 by CochraneItalia, Wiley Online Library on [15/10/2025]. See the Terms and Conditions (https://onlinelibrary.wiley.com/terms-and-conditions) on Wiley Online Library for rules of use; OA articles are governed by the applicable Creative Commons License

is one of the earliest phases in CM chondrites to be altered, as demonstrated by observations of alteration even in the least-altered (lowest petrographic grade) CM chondrites (e.g., Kimura et al., 2020; Palmer & Lauretta, 2011; Pignatelli et al., 2016, 2017). Whether type-I TCIs predate, overlap with, or post-date T1 calcite remains an open question. Conversely, T2 calcites formed later than both tochilinite and T1 calcites, either during or after the main phase of phyllosilicate growth and may have precipitated contemporaneously with the dense Fe-sulfides (pyrrhotite-troilite-pentlandite), as evidenced by the presence of these sulfide phases as inclusions in T2 calcite (Vacher et al., 2017). The magnetite measured for O-isotopes in this work was exclusively polyhedral magnetite. It shows a close association with dense Fe-sulfides (pentlandite) (Figure 2b) and we interpret these as magnetite pseudomorphically replacing sulfide in former pyrrhotite-pentlandite intergrowth masses, with the more resistant Ni-rich sulfides having survived. This type of replacement was well documented in Singerling and Brearley (2020) and demonstrates increasingly oxidizing conditions. The timing of this replacement is late in the alteration sequence because extensive magnetite formation and large magnetite masses are correlated with more advanced alteration (e.g., figure 7 in Howard et al., 2015 and Singerling & Brearley, 2020). Magnetite and tochilinite therefore cannot have formed at similar times.

Taken together, the petrographic evidence suggests that tochilinite (and particularly type-I TCIs) formed in closest temporal proximity to T1 calcite, in contrast to the later formed T2 calcite and magnetite. This close timing implies that the fluids from which they precipitated likely had similar isotopic compositions and temperatures. In the following section, we explore how the isotopic relationship between tochilinite and T1 calcite can offer further insight into the temperature of alteration on the CM parent body.

Section 2: Temperature During Tochilinite/T1 Calcite Formation—Assuming Equilibrium Conditions

Secondary minerals in carbonaceous chondrites preserve a "snapshot" of fluid evolution at the time of precipitation. However, the O-isotope composition of secondary minerals does not directly reflect the fluid from which they precipitated because different isotopes preferentially partition between the two phases (fluid and mineral). If the secondary minerals are in isotopic equilibrium with the fluid, then the equilibrium isotopic fractionation factor (α) quantifies the isotopic offset between the fluid and the precipitating mineral. Importantly, this fractionation factor is temperature-dependent. At higher temperatures, the partitioning effect is smaller because the enthalpy difference between isotopes becomes less significant as they acquire more kinetic energy (e.g., Urey, 1947; Watkins et al., 2013; Zheng, 2011). Consequently, the ambient temperature on the CM parent body at the time of secondary mineral formation can be reconstructed if (1) the fractionation factor (α) between the water and the target mineral has been accurately determined through experimental petrology and (2) the isotopic composition of the fluid at the time of mineral precipitation is known.

The problem is that, in most situations, we do not know the isotopic composition of the fluid at the time of mineral formation (the value $\delta^{18}O_{water}$ is unknown) and we are therefore forced to use an assumed value, and any reconstructed temperature estimates are therefore dependent on the accuracy of that assumption (e.g., Telus et al., 2019; Vacher, Piralla, et al., 2019; Verdier-Paoletti et al., 2017). Instead, this unknown can be avoided if we can demonstrate two independent secondary minerals precipitated in isotopic equilibrium (that is from the same fluid composition [$\delta^{18}O_{water}$] and temperature [T]). Under such an equilibrium scenario, the relative $\delta^{18}O$ fractionation between the two phases can be used to estimate the temperature of co-precipitation. This approach has previously been used in carbonaceous chondrites, for example between magnetite-carbonate associations in CR chondrites (Jilly-Rehak et al., 2018) and magnetite-dolomite associations in fine-grained micrometeorites (Dobrică et al., 2019).

Above, we argued that the similar timing of formation, trendline slope values close to a value of 0.52, and the close petrographic association between tochilinite and T1 calcite suggest that they likely formed from fluids with similar compositions and at similar temperatures. Building on this, in Section 2 we explore what temperature would be calculated under the assumption that these two phases formed in isotopic equilibrium. This approach requires well-constrained isotopic fractionation equations that describe the behavior of both mineral phases during precipitation.

(T1) Calcite Precipitation

The fractionation factor for calcite precipitation from water ($\alpha_{Calcite\text{-}Water}$) is well-characterized (e.g., Kim & O'Neil, 1997), largely due to its importance in paleoclimatology and paleotemperature reconstructions on Earth (e.g., Demeny et al., 2010; Zheng, 2011). We opted to use the experimentally constrained equilibrium isotopic fractionation factor for the calcite-water precipitation reaction from Kim and O'Neil (1997). This was derived for low temperatures (25–350°C) and terrestrial pressure conditions (1 bar), which is consistent with the conditions on the CM parent body. This work is perhaps the most widely used experimental equation, having been extensively applied over the last 27 years,

19455100, 2025, 10, Downloaded from https://onlinelibrary.wiley.com/doi/10.1111/maps.70043 by CochraneItalia, Wiley Online Library on [15/10/2025]. See the Terms and Conditions (https://onlinelibrary.wiley.com/terms-and-conditions) on Wiley Online Library for rules of use; OA articles are governed by the applicable Creative Commons License

including for hydrated C-type asteroid settings (e.g., Fujiya et al., 2020). Kim and O'Neil (1997) determined the following relationship:

$$10^3 \ln\alpha_{\text{Calcite-Water}} = 18.03 \cdot \left(\frac{10^3}{T}\right) - 32.42 \quad (1)$$

where T represents temperature (K) and $\alpha_{\text{Calcite-Water}}$ represents the equilibrium O-isotopic fractionation factor for calcite precipitation and is expressed as:

$$\alpha_{\text{Calcite-Water}} = \frac{^{18}\text{O}/^{16}\text{O}_{\text{Calcite}}}{^{18}\text{O}/^{16}\text{O}_{\text{Water}}} = \frac{1000 + \delta^{18}\text{O}_{\text{Calcite}}}{1000 + \delta^{18}\text{O}_{\text{Water}}} \quad (2)$$

We now have two unknowns: the O-isotope composition of the fluid at the time of calcite precipitation ($\delta^{18}O_{water}$), and the temperature at which the calcite formed (T), while the $\delta^{18}O_{calcite}$ value for T1 calcite we have measured using NanoSIMS (Table 2). The average value is $\delta^{18}O_{calcite} = 40.5 \pm 2.1‰$.

Tochilinite Precipitation

To date, no experimental fractionation factors have been determined for the precipitation of tochilinite from water. Nonetheless, because all of the oxygen present in tochilinite is held within the brucite-like metal-hydroxide layers (Mackinnon & Zolensky, 1984; Peng et al., 2009) we could apply a water-brucite fractionation factor and assume that the isotopic fractionation behavior for tochilinite is similar.

Brucite ($Mg(OH)_2$) is an end-member composition of the amakinite group and forms a solid solution with the Fe-rich end-member ($Fe(OH)_2$) sometimes called "ferroan brucite." The isotopic behavior of brucite precipitation from water at low temperatures (15–120 °C) and low pressures (1 bar)—relevant to the ambient conditions on the CM chondrite parent body (e.g., Suttle, King, et al., 2021) has been investigated by Xu and Zheng (1999). They determined the following relationship:

$$10^3 \ln\alpha_{\text{Brucite-Water}} = 1.56\left(10^6/T^2\right) - 14.1 \quad (3)$$

where T represents temperature (K) and $\alpha_{\text{Brucite-Water}}$ represents the equilibrium O-isotopic fractionation factor for the brucite precipitation reaction, expressed as:

$$\alpha_{\text{Brucite-Water}} = \frac{^{18}\text{O}/^{16}\text{O}_{\text{Brucite}}}{^{18}\text{O}/^{16}\text{O}_{\text{Water}}} = \frac{1000 + \delta^{18}\text{O}_{\text{Brucite}}}{1000 + \delta^{18}\text{O}_{\text{Water}}} \quad (4)$$

Xu and Zheng (1999) generated magnesium brucite with water over a range of aging times, fluid pH, and fluid compositions. Interestingly, they found that the O-isotope fractionation factor between brucite and water is independent of these variables. This implies that Equation (4) should be applicable to a ferroan brucite, although there is one limitation with this assumption; namely, that the stiffness of the Fe-OH bond is likely to be different from the Mg-OH bond (Schauble, 2004), owing to differences in atomic radius and electronegativities between these two cations (Fe and Mg). However, as the lattice configuration (oxidation state and coordination number of cations, plus the position of OH groups) is similar between magnesian and ferroan brucite, we assume the difference in fractionation between the two phases is sufficiently small to facilitate meaningful comparisons. This, by extension, permits Equation (3) to be used for the metal-hydroxide component within tochilinite.

We have measured the isotopic composition of the tochilinite ($\delta^{18}O_{tochilinite}$), with the average value given as $\delta^{18}O_{tochilinite} = 23.5 \pm 4.0‰$ (Table 2). Therefore, we have two unknowns, the O-isotope composition of the fluid ($\delta^{18}O_{water}$), and the temperature at which the tochilinite formed. However, because both these unknowns are the same unknowns as in Equation (1). The two equations (Equations 1 and 3) can be combined:

$$10^3 \ln\alpha_{\text{Tochilinite-Calcite}} = \frac{1.56 \cdot 10^6}{T^2} - \frac{18.03 \cdot 10^3}{T} + 18.32 \quad (5)$$

where $\alpha_{\text{Tochilinite-Calcite}}$ is given by:

$$\alpha_{\text{Tochilinite-Calcite}} = \frac{1000 + \delta^{18}\text{O}_{\text{Tochilinite}}}{1000 + \delta^{18}\text{O}_{\text{Calcite}}} \quad (6)$$

Substituting in our measured values for $\delta^{18}O_{tochilinite} = 23.5‰$ and $\delta^{18}O_{calcite} = 40.5‰$ gives $\alpha_{\text{Tochilinite-Calcite}}$ of approximately 0.9837 and a $10^3 \ln\alpha_{\text{Tochilinite-Calcite}}$ value of −16.47. Using Equation (5), substituting in the calculated value of $10^3 \ln\alpha_{\text{Tochilinite–Calcite}}$ and solving for temperature (T) requires rearranging into a quadratic expression:

$$x = \frac{-b \pm \sqrt{b^2 - 4ac}}{2a} \quad (7)$$

where: $x = 1/T$, $a = 1.56 \cdot 10^6$, $b = -18.03 \cdot 10^3$ and $c = 34.74$.

Solving this equation gives two possible solutions, −163°C and 135°C. Among these, −163°C is unrealistically low and can be discounted, while 135°C seems reasonable. However, this calculation only considered our average values for tochilinite and T1

19455100, 2025, 10, Downloaded from https://onlinelibrary.wiley.com/doi/10.1111/maps.70043 by CochraneItalia, Wiley Online Library on [15/10/2025]. See the Terms and Conditions (https://onlinelibrary.wiley.com/terms-and-conditions) on Wiley Online Library for rules of use; OA articles are governed by the applicable Creative Commons License

calcite. If instead the intrasample standard deviation is considered (i.e., tochilinite ±4.0‰ and T1 calcite ±2.1‰), then our temperature estimate expands. Specifically, the temperature solutions from these boundary values yield a minimum plausible temperature of 52°C and a maximum of 248°C.

Past laboratory experiments have demonstrated that tochilinite forms under alkaline conditions and over a temperature range from 80 to 320°C (Kozerenko et al., 2001). More recently, Vacher, Truche, et al. (2019) formed tochilinite in hydrothermal alteration experiments simulating conditions on the CM chondrite parent body. Based on an observed correlation between tochilinite cation composition (Fe/Mg ratio) they suggested that tochilinite in CM chondrites formed at temperatures of 120–160°C. This experiment hydrothermal synthesis-based estimate is in close agreement with our estimate from isotopic data; $T = 135$°C is very close to the median value of 140°C given by Vacher, Truche, et al. (2019). Together, these independent lines of evidence provide strong support for the approximate formation temperature of tochilinite.

For completeness, we should also consider the scenario for tochilinite and T2 calcite formation under isotopic equilibrium because this was partially supported by the statistical testing of our O-isotope data (Table 3) even though this seems unlikely based on existing petrographic knowledge for the progression of aqueous alteration and the relative timing of tochilinite and T2 calcite formation. If the above calculations are repeated but this time using our measured average T2 calcite value ($\delta^{18}O_{calcite} = 33.2‰$) this again gives two possible solutions, −170°C and 274°C. As before, the extremely negative temperature can be discounted. This temperature expands to a range ($155°C < T < 452°C$) if the intrasample standard deviations are also considered. In contrast to the T1 calcite scenario, the vast majority of this temperature range exceeds the stability field of tochilinite, as demonstrated from thermal decomposition experiments and studies of naturally heated meteorites, which suggest tochilinite decomposition occurs at temperatures above ~200°C (Fuchs et al., 1973; Jenkins et al., 2024; Zolensky, 1984). As a result, we conclude that tochilinite and T2 calcite co-precipitation is highly unlikely and instead the data better supports an equilibrium formation of tochilinite and T1 calcite.

Section 3: Temperature During Tochilinite/T1 Calcite Formation—Under Non-Equilibrium Conditions

In Section 2, we assumed that tochilinite and T1 calcite formed under isotopic equilibrium conditions. However, the analysis presented in Section 1 suggests that while this assumption is broadly reasonable, it is not strictly accurate. In Section 3, we therefore explore the alternative scenario in which tochilinite and T1 calcite formed under non-equilibrium conditions. As we have seen, under non-equilibrium conditions our mineral-specific fractionation equations have two unknowns, fluid composition ($\delta^{18}O_{water}$) and temperature (T). We can rearrange Equations (1) and (3) to make the fluid composition ($\delta^{18}O_{water}$) the subject, which for calcite appears as:

$$\delta^{18}O_{Water} = \frac{1000 + \delta^{18}O_{Calcite}}{e^{\left(\frac{18.03\cdot\left(\frac{10^3}{T}\right)-32.42}{10^3}\right)}} - 1000 \quad (8)$$

And for tochilinite appears as:

$$\delta^{18}O_{water} = \frac{1000 + \delta^{18}O_{Tochilinite}}{e^{\left(\frac{1.56\cdot10^3}{T^2}-0.0141\right)}} - 1000 \quad (9)$$

Next, by considering the relationship between the two unknowns and taking a range of potential temperatures, we can plot both equations on a single graph (Figure 4) allowing us to visualize the parameter space. On this plot, the intersection of the two curves represents the equilibrium isotopic fractionation conditions (those explored in Section 2), while any given condition where the curves do not intersect represents a non-equilibrium scenario. We know that, during aqueous alteration, the O-isotope composition of the parent body fluid evolved from high to low (e.g., Clayton & Mayeda, 1999). Therefore, we can conclude that temperatures lower than the intersection point (<135°C) require tochilinite to have formed before T1 calcite, while temperatures above the intersection point (>135°C) require tochilinite to have formed after T1 calcite. Unfortunately, based on the available evidence, we cannot make a further, more refined estimate of alteration temperatures (nor $\delta^{18}O_{water}$ compositions) but instead must leave the analysis at this point and wait for future data to resolve the potential possibilities. This might take the form of clear petrographic evidence demonstrating the relative sequence of mineralization between tochilinite (type-I TCIs) and T1 calcite, or additional tochilinite and/or T1 calcite measurements in other CM lithologies that more clearly demonstrate an isotopic equilibrium scenario.

CONCLUSIONS

We present new oxygen isotope data for CM chondrite parent body fluids, based on isotopic analyses of secondary phases (type-I tochilinite, T1 and T2 calcite, and magnetite) in the Winchcombe meteorite (lithology

19455100, 2025, 10, Downloaded from https://onlinelibrary.wiley.com/doi/10.1111/maps.70043 by CochraneItalia, Wiley Online Library on [15/10/2025]. See the Terms and Conditions (https://onlinelibrary.wiley.com/terms-and-conditions) on Wiley Online Library for rules of use; OA articles are governed by the applicable Creative Commons License

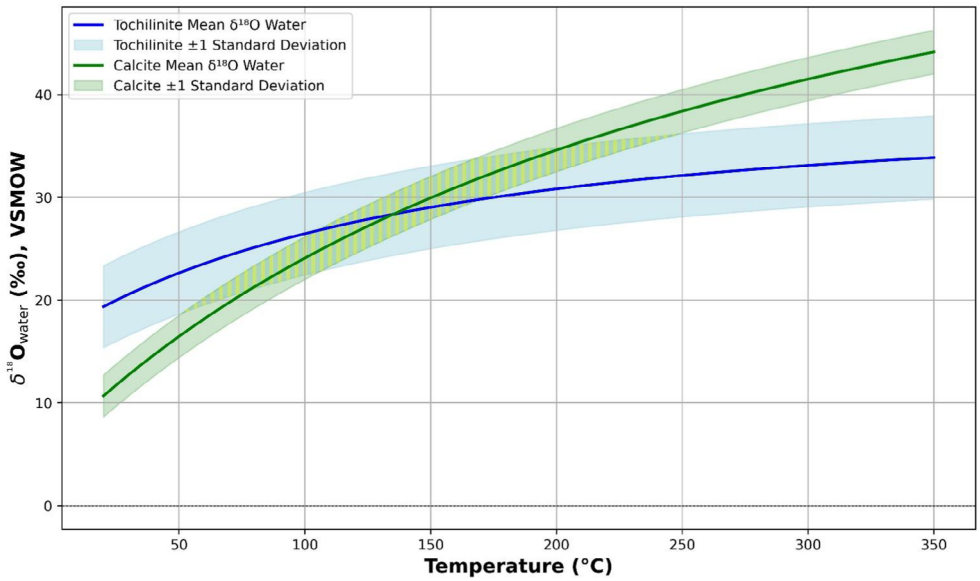

FIGURE 4. Comparing the inferred $\delta^{18}O_{Water}$ ranges for tochilinite (blue curve) and T1 calcite (green curve) over a potential alteration temperature range (25–350°C). The two curves intersect at $T = 135$°C and $\delta^{18}O_{Water} = 28‰$, representing the isotopic equilibrium condition. If the 1σ uncertainty arising from intrasample variation is considered (the shaded envelopes), then the potential ranges in temperature and $\delta^{18}O_{Water}$ are approximately $50 < T < 250$°C and $19 < \delta^{18}O_{Water} < 36‰$, respectively. (Color figure can be viewed at wileyonlinelibrary.com)

C, CM2.2/2.3). We begin by evaluating the distribution of O-isotopes in these secondary phases and show that, collectively, they define a linear trendline (slope 0.50) which is close to, but distinct from, a slope 0.52 line. This is interpreted as evidence of a complex fluid history during aqueous alteration. Specifically, this deviation reflects mass-independent mixing between ^{16}O-rich anhydrous silicates and ^{16}O-poor water, resulting in a progressive evolution in the $\Delta^{17}O$ composition of Winchcombe's fluids. At the same time, as secondary minerals precipitated, their isotopic signatures were governed by the instantaneous fluid composition but further modified by mineral-specific and temperature-dependent fractionation. Given that the observed slope of 0.50 is close to 0.52, we interpret mass-dependent processes as the dominant control on the isotopic behavior of Winchcombe's secondary phases.

Petrographic evidence indicates that tochilinite and T1 calcite are closely associated and likely formed at a similar, early stage in the alteration sequence. On this basis, we investigate the temperature and fluid composition given based on the assumption that both minerals formed in isotopic equilibrium, sharing the same $\Delta^{17}O$ value and temperature. This approach yields an estimated formation temperature of approximately 135°C and a $\delta^{18}O_{water}$ value of 28‰. This temperature value is in close agreement with the experimental hydrothermal synthesis of tochilinite under CM chondrite-like conditions by Vacher, Truche, et al. (2019), lending independent support to our interpretations.

Acknowledgments—We thank the Natural History Museum, London for the loan of a single Winchcombe section (P30423, accession number: BM.2022, M1-87). MDS was partially funded through internal departmental funds on a visiting fellow scheme at the University of Pisa, Dipartimento di Scienze della Terra. LF is supported by the Italian Ministry of Education, University and Research (MIUR) through research grants from the Programma Nazionale delle Ricerche in Antartide (grant number: PNRA16_00029). The Centro per l'Integrazione della Strumentazione scientifica dell'Università di Pisa (C.I.S.U.P.) is thanked for access to the single-crystal X-ray diffraction laboratory.

Conflict of Interest Statement—The authors declare no conflicts of interest.

Data Availability Statement—All data collected for this work is shown within the manuscript itself. There is no additional data that could be archived.

Editorial Handling—Dr. A. J. Timothy Jull

REFERENCES

Abreu, N. M., Aponte, J. C., Cloutis, E. A., and Nguyen, A. N. 2020. The Renazzo-Like Carbonaceous Chondrites as Resources to Understand the Origin, Evolution, and Exploration of the Solar System. *Geochemistry* 80: 125631.

Alexander, C. O. M. D., Greenwood, R. C., Bowden, R., Gibson, J. M., Howard, K. T., and Franchi, I. A. 2018. A

19455100, 2025, 10, Downloaded from https://onlinelibrary.wiley.com/doi/10.1111/maps.70043 by CochraneItalia, Wiley Online Library on [15/10/2025]. See the Terms and Conditions (https://onlinelibrary.wiley.com/terms-and-conditions) on Wiley Online Library for rules of use; OA articles are governed by the applicable Creative Commons License

Mutli-Technique Search for the most Primitive CO Chondrites. *Geochimica et Cosmochimica Acta* 221: 406–420.

Clayton, R. N., and Mayeda, T. K. 1999. Oxygen Isotope Studies of Carbonaceous Chondrites. *Geochimica et Cosmochimica Acta* 63: 2089–2104.

Daly, L., Suttle, M. D., Lee, M. R., Bridges, J., Hicks, L., Martin, P. E. M., Floyd, C. J., et al. 2024. Brecciation at the Grain Scale within the Lithologies of the Winchcombe Mighei-Like Carbonaceous Chondrite. *Meteoritics & Planetary Science* 59: 1068–1100.

Demeny, A., Kele, S., and Siklósy, Z. 2010. Empirical Equations for the Temperature Dependence of Calcite-Water Oxygen Isotope Fractionation from 10 to 70° C. *Rapid Communications in Mass Spectrometry* 24: 3521–26.

Dietze, F., and Kontny, A. 2003. A Study of Rock Magnetic Properties of Serpentinites from the Outokumpu Deep Drill Hole, Finland. *Outokumpu Deep Drilling Project* 2010: 133–150.

Dobrică, E., Ogliore, R. C., Engrand, C., Nagashima, K., and Brearley, A. J. 2019. Mineralogy and Oxygen Isotope Systematics of Magnetite Grains and a Magnetite-Dolomite Assemblage in Hydrated Fine-Grained Antarctic Micrometeorites. *Meteoritics & Planetary Science* 54: 1973–89.

Fan, Y., Li, S., Liu, S., Yin, Q., Song, G., Xu, R., Zhang, J., et al. 2022. Shidian Meteorite, a New Fall Analog of Near-Earth Asteroid (101955) Bennu. *Meteoritics & Planetary Science* 57: 2192–2215.

Farver, J. R. 1994. Oxygen Self-Diffusion in Calcite: Dependence on Temperature and Water Fugacity. *Earth and Planetary Science Letters* 121: 575–587.

Fuchs, L. H., Olsen, E., and Jensen, K. J. 1973. Mineralogy, Mineral- Chemistry, and Composition of the Murchison (C2) Meteorite. *Smithsonian Contributions to the Earth Sciences* 10: 1–39.

Fujiya, W. 2018. Oxygen Isotopic Ratios of Primordial Water in Carbonaceous Chondrites. *Earth and Planetary Science Letters* 481: 264–272.

Fujiya, W., Aoki, Y., Ushikubo, T., Hashizume, K., and Yamaguchi, A. 2020. Carbon Isotopic Evolution of Aqueous Fluids in CM Chondrites: Clues from In-Situ Isotope Analyses within Calcite Grains in Yamato-791198. *Geochimica et Cosmochimica Acta* 274: 246–260.

Greenwood, R. C., Findlay, R., Martins, R., Steele, R. C. J., Shaw, K. M. M., Morton, E., Savage, P. S., et al. 2024. The Formation and Aqueous Alteration of CM2 Chondrites and their Relationship to CO3 Chondrites: A Fresh Isotopic (O, Cd, Cr, Si, Te, Ti, and Zn) Perspective from the Winchcombe CM2 Fall. *Meteoritics & Planetary Science* 59: 1170–93.

Greenwood, R. C., Franchi, I. A., Findlay, R., Malley, J. A., Ito, M., Yamaguchi, A., Kimura, M., et al. 2023. Oxygen Isotope Evidence from Ryugu Samples for Early Water Delivery to Earth by CI Chondrites. *Nature Astronomy* 7: 29–38.

Gubaidulina, T. V., Chistyakova, N. I., and Rusakov, V. S. 2007. Mössbauer Study of Layered Iron Hydroxysulfides: Tochilinite and Valleriite. *Bulletin of the Russian Academy of Sciences: Physics* 71: 1269–72.

Hauri, E. H., Papineau, D., Wang, J., and Hillion, F. 2016. High-Precision Analysis of Multiple Sulfur Isotopes Using NanoSIMS. *Chemical Geology* 420: 148–161.

Howard, K. T., Alexander, C. O. D., Schrader, D. L., and Dyl, K. A. 2015. Classification of Hydrous Meteorites (CR, CM and C2 Ungrouped) by Phyllosilicate Fraction: PSD-XRD Modal Mineralogy and Planetesimal Environments. *Geochimica et Cosmochimica Acta* 149: 206–222.

Jenkins, L. E., King, A. J., Lee, M. R., Daly, L., Thompson, S. P., Day, S. J., Saunders, L., Martin, P. E., and Bintang, F. 2024. A High-Resolution In Situ X-Ray Diffraction Study of Mineral Transitions Due to Post-Hydration Heating in CM Chondrite Meteorites. *Earth, Planets and Space* 76: 172.

Jilly-Rehak, C. E., Huss, G. R., Nagashima, K., and Schrader, D. L. 2018. Low-Temperature Aqueous Alteration on the CR Chondrite Parent Body: Implications from In Situ Oxygen-Isotope Analyses. *Geochimica et Cosmochimica Acta* 222: 230–252.

Kakos, G. A., Turney, T. W., and Williams, T. B. 1994. Synthesis and Structure of Tochilinite: A Layered Metal Hydroxide/Sulfide Composite. *Journal of Solid State Chemistry* 108: 102–111.

Kim, S. T., and O'Neil, J. R. 1997. Equilibrium and Nonequilibrium Oxygen Isotope Effects in Synthetic Carbonates. *Geochimica et Cosmochimica Acta* 61: 3461–75.

Kimura, M., Imae, N., Komatsu, M., Barrat, J. A., Greenwood, R. C., Yamaguchi, A., and Noguchi, T. 2020. The most Primitive CM Chondrites, Asuka 12085, 12169, and 12236, of Subtypes 3.0–2.8: Their Characteristic Features and Classification. *Polar Science* 26: 100565.

King, A. J., Daly, L., Rowe, J., Joy, K. H., Greenwood, R. C., Devillepoix, H. A., Suttle, M. D., et al. 2022. The Winchcombe Meteorite, a Unique and Pristine Witness from the Outer Solar System. *Science Advances* 8: eabq3925.

King, A. J., Russell, S. S., Schofield, P. F., Humphreys-Williams, E. R., Strekopytov, S., Abernethy, F. A. J., Verchovsky, A. B., and Grady, M. M. 2019. The Alteration History of the Jbilet Winselwan CM Carbonaceous Chondrite: An Analog for C-Type Asteroid Sample Return. *Meteoritics & Planetary Science* 54: 521–543.

King, A. J., Schofield, P. F., and Russell, S. S. 2017. Type 1 Aqueous Alteration in CM Carbonaceous Chondrites: Implications for the Evolution of Water-Rich Asteroids. *Meteoritics & Planetary Science* 52: 1197–1215.

Kozerenko, S. V., Fadeev, V. V., Organova, N. I., Chstyakova, N. I., Kolpakova, N. N., and Senin, V. G. 2001. Synthesis, Formation Conditions and Crystallochemistry of Tochilinites-Iron, Magnesium and Sodium Hydroxide-Sulfides. *Experiment In Geosciences* 10: 57–58.

Lee, M. R., Cohen, B. E., King, A. J., and Greenwood, R. C. 2019. The Diversity of CM Carbonaceous Chondrite Parent Bodies Explored Using Lewis Cliff 85311. *Geochimica et Cosmochimica Acta* 264: 224–244.

Lee, M. R., Lindgren, P., King, A. J., Greenwood, R. C., Franchi, I. A., and Sparkes, R. 2016. Elephant Moraine 96029, a Very Mildly Aqueously Altered and Heated CM Carbonaceous Chondrite: Implications for the Drivers of Parent Body Processing. *Geochimica et Cosmochimica Acta* 187: 237–259.

Lee, M. R., Lindgren, P., and Sofe, M. R. 2014. Aragonite, Breunnerite, Calcite and Dolomite in the CM Carbonaceous Chondrites: High Fidelity Recorders of Progressive Parent Body Aqueous Alteration. *Geochimica et Cosmochimica Acta* 144: 126–156.

19455100, 2025, 10, Downloaded from https://onlinelibrary.wiley.com/doi/10.1111/maps.70043 by CochraneItalia, Wiley Online Library on [15/10/2025]. See the Terms and Conditions (https://onlinelibrary.wiley.com/terms-and-conditions) on Wiley Online Library for rules of use; OA articles are governed by the applicable Creative Commons License

Lee, M. R., Sofe, M. R., Lindgren, P., Starkey, N. A., and Franchi, I. A. 2013. The Oxygen Isotope Evolution of Parent Body Aqueous Solutions as Recorded by Multiple Carbonate Generations in the Lonewolf Nunataks 94101 CM2 Carbonaceous Chondrite. *Geochimica et Cosmochimica Acta* 121: 452–466.

Lentfort, S., Bischoff, A., Ebert, S., and Patzek, M. 2021. Classification of CM Chondrite Breccias—Implications for the Evaluation of Samples from the OSIRIS-rex and Hayabusa 2 Missions. *Meteoritics & Planetary Science* 56: 127–147.

Lindgren, P., Lee, M. R., Starkey, N. A., and Franchi, I. A. 2017. Fluid Evolution in CM Carbonaceous Chondrites Tracked Through the Oxygen Isotopic Compositions of Carbonates. *Geochimica et Cosmochimica Acta* 204: 240–251.

Mackinnon, I. D., and Zolensky, M. E. 1984. Proposed Structures for Poorly Characterized Phases in C2M Carbonaceous Chondrite Meteorites. *Nature* 309: 240–42.

McSween, H. Y., Jr. 1987. Aqueous Alteration in Carbonaceous Chondrites: Mass Balance Constraints on Matrix Mineralogy. *Geochimica et Cosmochimica Acta* 51: 2469–77.

Miller, M. F., Franchi, I. A., Sexton, A. S., and Pillinger, C. T. 1999. High Precision δ17O Isotope Measurements of Oxygen from Silicates and Other Oxides: Method and Applications. *Rapid Communications in Mass Spectrometry* 13: 1211–17.

Moriarty, G. M., Rumble, D., III, and Friedrich, J. M. 2009. Compositions of Four Unusual CM or CM-Related Antarctic Chondrites. *Geochemistry* 69: 161–68.

Muramatsu, Y., and Nambu, M. 1980. Tochilinite and Cuprian Tochilinite from the Kamaishi Mine, Iwate Prefecture, Japan. *The Journal of the Japanese Association of Mineralogists, Petrologists and Economic Geologists* 75: 377–384.

Nakamura, T., Matsumoto, M., Amano, K., Enokido, Y., Zolensky, M. E., Mikouchi, T., Genda, H., et al. 2022. Formation and Evolution of Carbonaceous Asteroid Ryugu: Direct Evidence from Returned Samples. *Science* 379: eabn8671.

Organova, N. I., Gorshkov, A. I., Dikov, Y. P., Kul'Bachinskiy, V. A., Laputina, I. P., Sivtsov, A. V., Sluzhenikin, S. F., and Ponomarenko, A. I. 1988. New Data on Tochilinite. *International Geology Review* 30: 691–705.

Palmer, E. E., and Lauretta, D. S. 2011. Aqueous Alteration of Kamacite in CM Chondrites. *Meteoritics & Planetary Science* 46: 587–1607.

Peng, Y., Xi, G., Zhong, C., Wang, L., Lu, J., Sun, X., Zhu, L., et al. 2009. An Experimental Study on the Preparation of Tochilinite-Originated Intercalation Compounds Comprised of Fe1−xS Host Layers and Various Kinds of Guest Layers. *Geochimica et Cosmochimica Acta* 73: 4862–78.

Pignatelli, I., Marrocchi, Y., Mugnaioli, E., Bourdelle, F., and Gounelle, M. 2017. Mineralogical, Crystallographic and Redox Features of the Earliest Stages of Fluid Alteration in CM Chondrites. *Geochimica et Cosmochimica Acta* 209: 106–122.

Pignatelli, I., Marrocchi, Y., Vacher, L. G., Delon, R., and Gounelle, M. 2016. Multiple Precursors of Secondary Mineralogical Assemblages in CM Chondrites. *Meteoritics & Planetary Science* 51: 785–805.

Pouchou, J. L., and Pichoir, F. 1991. Quantitative Analysis of Homogeneous or Stratified Microvolumes Applying the Model "PAP". In *Electron Probe Quantitation*, edited by K. F. J. Heinrich, and D. E. Newbury, 31–75. New York, NY: Springer.

Riciputi, L. R., Paterson, B. A., and Ripperdan, R. L. 1998. Measurement of Light Stable Isotope Ratios by SIMS: Matrix Effects for Oxygen, Carbon, and Sulfur Isotopes in Minerals. *International Journal of Mass Spectrometry* 178: 81–112.

Rubin, A. E., Trigo-Rodríguez, J. M., Huber, H., and Wasson, J. T. 2007. Progressive Aqueous Alteration of CM Carbonaceous Chondrites. *Geochimica et Cosmochimica Acta* 71: 2361–82.

Russell, S. S., King, A. J., Bates, H. C., Almeida, N. V., Greenwood, R. C., Daly, L., Joy, K. H., et al. 2024. Recovery and Curation of the Winchcombe (CM2) Meteorite. *Meteoritics & Planetary Science* 59(5): 973–987.

Sakamoto, N., Seto, Y., Itoh, S., Kuramoto, K., Fujino, K., Nagashima, K., Krot, A. N., and Yurimoto, H. 2007. Remnants of the Early Solar System Water Enriched in Heavy Oxygen Isotopes. *Science* 317: 231–33.

Sandström, F. 2012. Otamo dolomitbrott i Siikainen, Finland. *Litofilen. Medlemsblad för Västerås AmatörGeologiska Sällskap* 29: 23–38.

Schauble, E. A. 2004. Applying Stable Isotope Fractionation Theory to New Systems. *Reviews in Mineralogy and Geochemistry* 55: 65–111.

Scicchitano, M. R., Rubatto, D., Hermann, J., Shen, T., Padrón-Navarta, J. A., Williams, I. S., and Zheng, Y. F. 2018. In Situ Oxygen Isotope Determination in Serpentine Minerals by Ion Microprobe: Reference Materials and Applications to Ultrahigh-Pressure Serpentinites. *Geostandards and Geoanalytical Research* 42: 459–479.

Singerling, S. A., and Brearley, A. J. 2020. Altered Primary Iron Sulfides in CM 2 and CR 2 Carbonaceous Chondrites: Insights into Parent Body Processes. *Meteoritics & Planetary Science* 55: 496–523.

Suttle, M. D., Daly, L., Jones, R. H., Jenkins, L., Van Ginneken, M., Mitchell, J. T., Bridges, J. C., et al. 2024. The Winchcombe Meteorite—A Regolith Breccia from a Rubble Pile CM Chondrite Asteroid. *Meteoritics & Planetary Science* 59: 1043–67.

Suttle, M. D., Greshake, A., King, A. J., Schofield, P. F., Tomkins, A., and Russell, S. S. 2021. The Alteration History of the CY Chondrites, Investigated through Analysis of a New Member: Dhofar 1988. *Geochimica et Cosmochimica Acta* 295: 286–309.

Suttle, M. D., King, A. J., Schofield, P. F., Bates, H., and Russell, S. S. 2021. The Aqueous Alteration of CM Chondrites, a Review. *Geochimica et Cosmochimica Acta* 299: 219–256.

Telus, M., Hauri, E. H., and Wang, J. 2019. Calcite and Dolomite Formation in the CM Parent Body: Insight from In Situ C and O Isotope Analyses. *Geochimica et Cosmochimica Acta* 260: 275–291.

The Meteoritical Bulletin. 2024. Online Accessed 01/07/2024. https://www.lpi.usra.edu/meteor/.

Tomeoka, K., and Buseck, P. R. 1985. Indicators of Aqueous Alteration in CM Carbonaceous Chondrites: Microtextures of a Layered Mineral Containing Fe, S, O and Ni. *Geochimica et Cosmochimica Acta* 49: 2149–63.

Tomkinson, T. O. R. 2012. Constraining the Formation Conditions of the Ancient Martian ALH 84001 Carbonates. PhD Thesis. Open University (United Kingdom). https://oro.open.ac.uk/61122/1/590812.pdf.

19455100, 2025, 10, Downloaded from https://onlinelibrary.wiley.com/doi/10.1111/maps.70043 by CochraneItalia, Wiley Online Library on [15/10/2025]. See the Terms and Conditions (https://onlinelibrary.wiley.com/terms-and-conditions) on Wiley Online Library for rules of use; OA articles are governed by the applicable Creative Commons License

Tyra, M., Brearley, A., and Guan, Y. 2016. Episodic Carbonate Precipitation in the CM Chondrite ALH 84049: An Ion Microprobe Analysis of O and C Isotopes. *Geochimica et Cosmochimica Acta* 175: 195–207.

Tyra, M. A., Farquhar, J., Wing, B. A., Benedix, G. K., Jull, A. J. T., Jackson, T., and Thiemens, M. H. 2007. Terrestrial Alteration of Carbonate in a Suite of Antarctic CM Chondrites: Evidence from Oxygen and Carbon Isotopes. *Geochimica et Cosmochimica Acta* 71: 782–795.

Urey, H. C. 1947. The Thermodynamic Properties of Isotopic Substances. *Journal of the Chemical Society (Resumed)*: 562–581. https://doi.org/10.1039/JR9470000562

Ushikubo, T., Kimura, M., Kita, N. T., and Valley, J. W. 2012. Primordial Oxygen Isotope Reservoirs of the Solar Nebula Recorded in Chondrules in Acfer 094 Carbonaceous Chondrite. *Geochimica et Cosmochimica Acta* 90: 242–264.

Vacher, L. G., Marrocchi, Y., Villeneuve, J., Verdier-Paoletti, M. J., and Gounelle, M. 2017. Petrographic and C & O Isotopic Characteristics of the Earliest Stages of Aqueous Alteration of CM Chondrites. *Geochimica et Cosmochimica Acta* 213: 271–290.

Vacher, L. G., Piralla, M., Gounelle, M., Bizzarro, M., and Marrocchi, Y. 2019. Thermal Evolution of Hydrated Asteroids Inferred from Oxygen Isotopes. *The Astrophysical Journal* 882: L20.

Vacher, L. G., Truche, L., Faure, F., Tissandier, L., Mosser-Ruck, R., and Marrocchi, Y. 2019. Deciphering the Conditions of Tochilinite and Cronstedtite Formation in CM Chondrites from Low Temperature Hydrothermal Experiments. *Meteoritics & Planetary Science* 54: 1870–89.

Van de Vusse, R., and Powell, R. 1983. The Interpretation of Pyrrhotine-Pentlandite-Tochilinite-Magnetite-Magnesite Textures in Serpentinites from Mount Keith, Western Australia. *Mineralogical Magazine* 47: 501–5.

Verdier-Paoletti, M. J., Marrocchi, Y., Avice, G., Roskosz, M., Gurenko, A., and Gounelle, M. 2017. Oxygen Isotope Constraints on the Alteration Temperatures of CM Chondrites. *Earth and Planetary Science Letters* 458: 273–281.

Verdier-Paoletti, M. J., Marrocchi, Y., Vacher, L. G., Gattacceca, J., Gurenko, A., Sonzogni, C., and Gounelle, M. 2019. Testing the Genetic Relationship between Fluid Alteration and Brecciation in CM Chondrites. *Meteoritics & Planetary Science* 54: 1692–1709.

Watkins, J. M., Nielsen, L. C., Ryerson, F. J., and DePaolo, D. J. 2013. The Influence of Kinetics on the Oxygen Isotope Composition of Calcium Carbonate. *Earth and Planetary Science Letters* 375: 349–360.

Xu, B. L., and Zheng, Y. F. 1999. Experimental Studies of Oxygen and Hydrogen Isotope Fractionations between Precipitated Brucite and Water at Low Temperatures. *Geochimica et Cosmochimica Acta* 63: 2009–18.

Yurimoto, H., Kuramoto, K., Krot, A. N., Scott, E. R. D., Cuzzi, J. N., Thiemens, M. H., and Lyons, J. R. 2007. Origin and Evolution of Oxygen Isotopic Compositions of the Solar System. In *Protostars and Planets*, edited by V. V. B. Reipurth, D. Jewitt, and K. Keil, 849–862. University of Arizona Press, 951.

Zheng, Y. F. 2011. On the Theoretical Calculations of Oxygen Isotope Fractionation Factors for Carbonate-Water Systems. *Geochemical Journal* 45: 341–354.

Zolensky, M. E. 1984. Hydrothermal Alteration of CM Carbonaceous Chondrites; Implications of the Identification of Tochilinite as One Type of Meteoritic PCP 47th Annual Meeting of the Meteoritical Society, vol. 537, p. 19.

Zolensky, M. E., and Mackinnon, I. D. 1986. Microstructures of Cylindrical Tochilinites. *American Mineralogist* 71: 1201–9.

SUPPORTING INFORMATION

Additional supporting information may be found in the online version of this article.

Table S1. X-ray diffraction pattern of tochilinite from the Otamo quarry.

Table S2. Bulk CM chondrite data extracted from the literature and used in this work to plot the shaded region in Figure 3.

Figure S1. Raman spectra comparing tochilinite in Winchcombe to a terrestrial tochilinite standard (from the RRUFF database).

Figure S2. SEM BSE images of the measured tochilinite grain in this study.

Figure S3. SEM BSE images of the measured T1 and T2 carbonates in this study.

19455100, 2025, 10, Downloaded from https://onlinelibrary.wiley.com/doi/10.1111/maps.70043 by CochraneItalia, Wiley Online Library on [15/10/2025]. See the Terms and Conditions (https://onlinelibrary.wiley.com/terms-and-conditions) on Wiley Online Library for rules of use; OA articles are governed by the applicable Creative Commons License